EurJIC European Journal of Inorganic Chemistry

ChemPubSoc Europe

FULL PAPER

DOI:10.1002/ejic.201500489

Colorimetric Detection of Spermine by the Cu^{II} Complex of Imine-Based Organic Nanoaggregates in Aqueous Medium

Shweta Chopra,[a][‡] Jasminder Singh,[b][‡] Harpreet Kaur,[a] Ajnesh Singh,[b] Narinder Singh,*[b] and Navneet Kaur*[a]

Keywords: Colorimetry / Sensors / Biogenic amines / Nanoparticles / Schiff bases / Copper

A Schiff-base receptor bearing different functionalities was synthesized from dipicolinic acid hydrazide and characterized with several spectroscopic techniques. To explore its practical application as a sensor, the receptor was processed into organic nanoaggregates (**O1**) in aqueous medium by the reprecipitation method. The **O1** nanoaggregates were characterized by techniques such as dynamic light scattering and TEM, and their recognition properties for metal ions were investigated by fluorescence spectroscopy. The nanoaggregates showed selectivity for Cu^{2+} over other metal ions. The structure of the complex **O1**·Cu^{2+} thus formed was determined by single-crystal X-ray crystallography. Complex **O1**·Cu^{2+} was further employed as a sensor for detection of biogenic amines in aqueous medium, and showed selective sensing of spermine with a detection limit of 7.62 nM. The color change on addition of spermine to the complex can be seen with the naked eye. Moreover, stability in the physiological pH range and negligible effect of ionic environment provided the opportunity for real-time application of the sensor in aqueous medium.

Introduction

Biogenic amines (BAs) are low molecular weight biomolecules and can be categorized as aliphatic (e.g., spermine, spermidine), aromatic (e.g., tyramine, phenylethylamine), and heterocyclic (e.g., histamine, tryptamine) organic bases. BAs are found as physiological components of several food products and are also generated by decarboxylation of amino acids present in the food by bacterial action. In other words, the origin of BAs can be categorized as endogenous or exogenous.[1–3] In the human body BAs are formed by various metabolic process and are necessary in diverse physiological functions. For example, spermine and spermidine regulate growth, serotonin acts as a neural transmitter, histamine and tyramine are inflammation agents, and BAs are involved in cell-membrane equilibrium, cell propagation, and the synthesis of RNA, DNA, and various proteins.[4–6] Hence, BAs are of great physiological importance and pose no threat to human health if present in permissible limits, but when present in excess they pose a serious threat to human health, as several BAs have numerous toxicological repercussions. For example, histamine, tyramine, and phenylethylamine can cause a variety of symptoms in the human body, such as nausea, rashes, abdominal cramps, itching, burning, tingling, and hypotension. Putrescine and cadaverine are secondary amines that cause food poisoning by enhancing the physiological effect of histamine. Tyramine is also considered to cause hypertension.[7–9] The amount of BA present in foodstuffs is used as a quality index for their storage and to check for spoilage. Considering the extent of physiological and health effects caused by these BAs, their determination in various foodstuffs, especially before packaging, is of major importance.[10] Various methods are available in the literature for determination of amines, such as HPLC, electrophoresis, and electrochemical techniques. These techniques require expert handling and laborious interpretation.[8,11–13] On the other hand, techniques such as UV/Vis absorption and fluorescence spectroscopy do not require expert handling or preparation of solutions.[14,15] Various receptors have been devised for determination of biomolecules that form hydrogen bonds with the receptors, but their use in aqueous medium is a challenge owing to formation of hydrogen bonds with water molecules instead of biomolecules.[16] However, complexation of metal ions with the receptor provides a suitable alternative to determination through hydrogen bonding, as it brings electrostatic interactions of complexes with biomolecules into the picture.[17]

[a] Centre for Nanoscience and Nanotechnology (UIEAST), Panjab University,
Chandigarh 160014, India
E-mail: navneetkaur@pu.ac.in
www.puchd.ac.in
[b] Department of Chemistry, Indian Institute of Technology Ropar (IIT Ropar),
Rupnagar, Panjab 140001, India
E-mail: nsingh@iitrpr.ac.in
www.iitrpr.ac.in
[‡] Both authors contributed equally.
Supporting information for this article is available on the WWW under http://dx.doi.org/10.1002/ejic.201500489.

Keeping these perspectives in view, we synthesized receptor **1** and converted it to organic nanoaggregates **O1** by a single-step reprecipitation method. These organic nanoaggregates show good optical fluorescence properties and form complexes selectively with copper ions. The complex **O1**·Cu^{2+} was used for analytical determination of BAs with detection by UV/Vis absorption spectroscopy and the naked eye.

Results and Discussion

Synthetic Procedure

Receptor **1** was obtained by condensation of dipicolinic acid hydrazide[18] with salicylaldehyde in ethanol (Scheme 1). The structure was confirmed by ^{1}H and ^{13}C NMR spectroscopy, IR spectroscopy, CHN analysis, and mass spectrometry (Figures S1–S4).

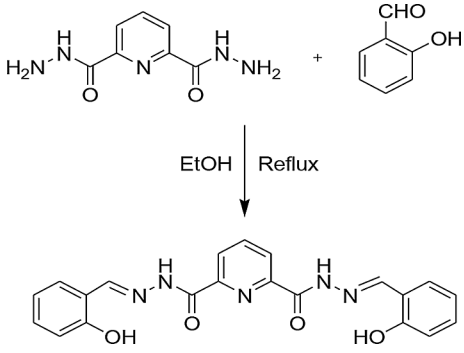

Scheme 1. Synthesis of receptor **1**.

Nanoaggregate Formation

The practical applications of organic nanoparticles in advanced materials for, for example, drugs, display elements, and cosmetics, which are due to their excellent solubility in water and biodegradable nature, have opened great perspectives in the fields of biology and green chemistry.[19–21] Their size domain, which is quite different from that of inorganic nanomaterials, ranges from a few tens of nanometers to a few hundred nanometers. The optical properties of nanoparticles of molecules with flexible conformation are size-dependent. Therefore, fabrication of organic nanoaggregates of requisite size is of the utmost importance. Herein, we utilized a single-step reprecipitation process for the fabrication of organic nanoparticles.[22] This process was carried out by time-regulated injection of a solution of receptor **1** in DMF to doubly-distilled water (100 mL) with sonication, which led to aggregation of receptor **1** and dispersion of nanoaggregates **O1**. Various solvent/water systems were tried for nanoaggregation; the requisite size was obtained with water/DMF (99/1, v/v). The formation of **O1** was confirmed by dynamic light scattering (DLS) and TEM, which showed a narrow size distribution around 15 nm (Figure 1). The fluorescence spectrum of **O1** in aqueous solution showed marked differences to the emission profile of receptor **1** in an organic solution. Nanoaggregates **O1** are highly fluorescent at 515 nm, in contrast to their predecessor **1**, when excited at 353 nm (Figure 2). The ob-

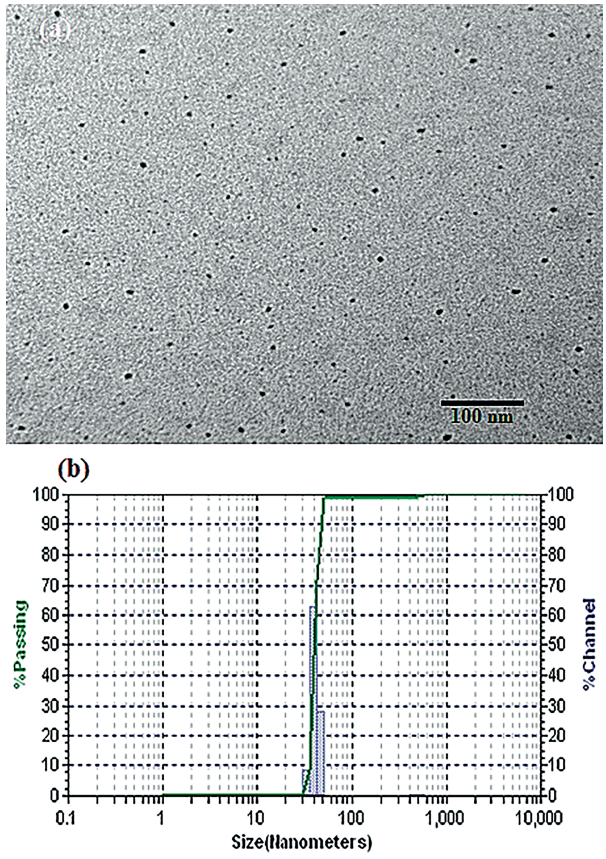

Figure 1. (a) TEM image and (b) DLS size distribution of nanoaggregates of receptor **1** prepared in aqueous solution.

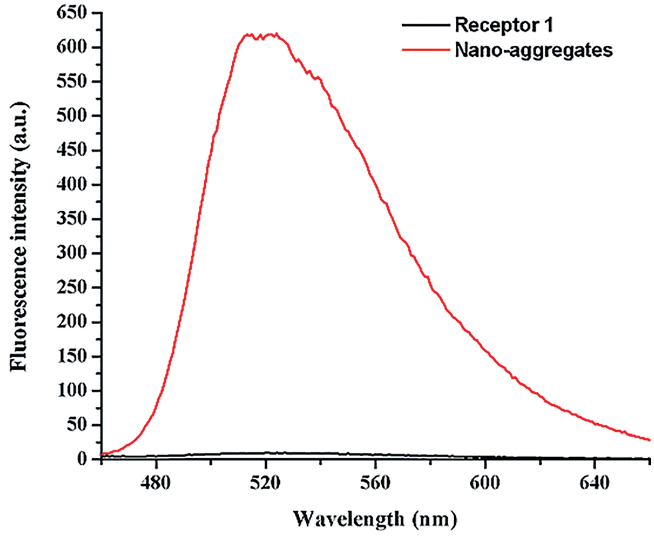

Figure 2. Emission profile of nanoaggregate **O1** in DMF/water (1:99, v/v) and receptor **1** in DMF.

served differences are in accordance with aggregation-induced emission.[23,24]

Fluorescent Recognition of Cu^{2+}

The binding ability of **O1** with different metal ions was tested. Fluorometric analysis of various metal ions (Li^+, Na^+, K^+, Cs^+, Mg^{2+}, Ca^{2+}, Sr^{2+}, Ba^{2+}, Al^{3+}, Cr^{3+}, Mn^{2+}, Fe^{3+}, Co^{3+}, Cu^{2+}, Zn^{2+}, Ag^+, Cd^{2+}, Pb^{2+}, Hg^{2+}; 50 μM each) as their nitrate salts revealed that **O1** (10 μM) can bind Cu^{2+} ions selectively with fluorescence turn-off behavior (Figure S5). To authenticate **O1** as potential sensor for copper ions, quantitative titration was performed by addition of small aliquots of copper nitrate solution to a solution of **O1**, which resulted in uniform quenching of fluorescence intensity with good linearity in the range 0–70 μM, with a lower detection limit of 7.9 nM, calculated by the 3σ method.[25] The fluorescence quenching can be attributed to complexation of **O1** and Cu^{2+} in aqueous medium (Figure S6). Moreover, this quenching activity could be explained partly by considering the paramagnetic nature of copper ions and partly by coordination of Cu^{2+} with donor atoms of **1**, which inhibits the charge-transfer process. The structure of the complex formed between receptor **1** and copper nitrate was fully characterized by single-crystal XRD. To further authenticate the exclusive binding of copper ion with the receptor, competitive binding was performed (Figure S7), which revealed that that copper binds exclusively with receptor **1** without any interference from other metal ions.

Structure Description

The copper complex of **1** crystallizes in the triclinic crystal system with space group $P\bar{1}$. The asymmetric unit consists of one molecule of the complex and three DMF molecules as solvent of crystallization. The ORTEP with atom-numbering scheme is shown in Figure 3.

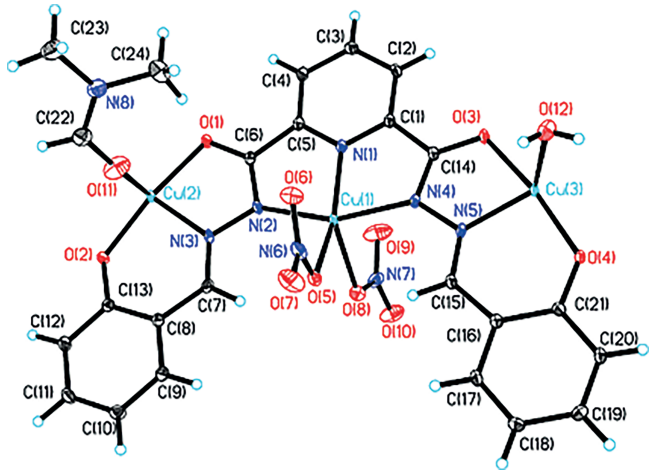

Figure 3. ORTEP of the copper complex of **1** with 40% probability thermal ellipsoids and atom-numbering scheme (solvent molecules of crystallization are omitted for clarity).

The complex is a 1D coordination polymer in which tris-Cu^{II} units are repeated along the *bc* plane (Figure 4). The coordination around Cu(1) is trigonal-bipyramidal with ligation by three donor nitrogen atoms of **1** and two monodentate nitrate ions. The other two copper ions, Cu(2) and Cu(3), have square-pyramidal geometries. The five coordination sites of Cu(2) are filled by three oxygen and one nitrogen atoms of ligand **1** and one oxygen atom of a coordinated DMF ligand. The Cu(3) center has similar coordination to Cu(2), but here the fifth coordination site is occupied by a coordinated water molecule. Selected bond lengths and angles around the metal centers are listed in Table S2.

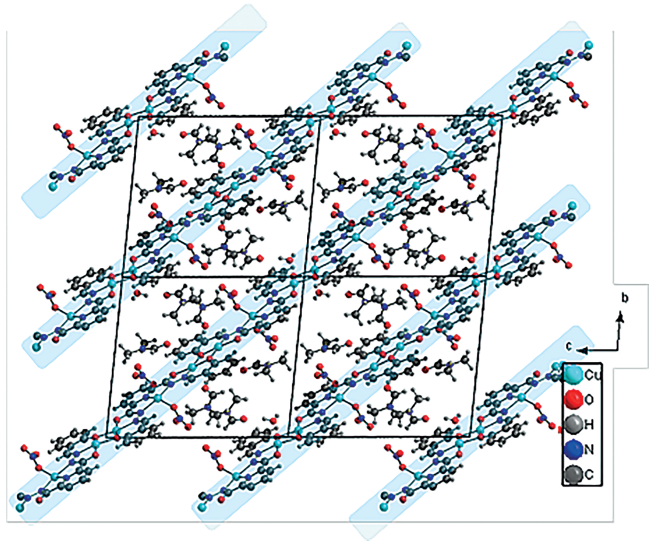

Figure 4. Packing diagram of the copper complex viewed down the *a*-axis.

When the packing of the complex is viewed down the *a*-axis (Figure 4), a layered arrangement can be seen. These layers are formed by 1D chains of the complex. The vacant spaces between the 1D chains are filled by solvent molecules of crystallization. These solvent molecules interact with each other and the 1D chains through extensive hydrogen bonding (i.e., O–H···O and C–H···O/N hydrogen bonds). The hydrogen-bonding parameters are listed in Table S3. No other significant π–π stacking or C–H···π interactions were observed.

Recognition Study with BAs

The binding selectivity of **O1**·Cu^{2+} toward eight important BAs (spermine, spermidine, tyramine, 2-phenylethylamine, histamine, 1,2-diaminopropane, 1,4-diaminobutane, and 1,5-diaminopentane; 100 μM each) in aqueous medium was determined by UV/Vis spectrophotometry. The absorption spectrum exhibited a significant decrease in absorbance at 397 nm and the appearance of new peak at 551 nm in the presence of spermine, and had clear isosbestic point at 439 nm during the titration experiment (Figure 5, a and b). Whereas minor changes were produced by the other BAs, the change in absorption behavior due to spermine resulted in a color change of the **O1**·Cu^{2+} solution from yellow to

blue, which can be used for naked-eye detection of spermine with **O1**·Cu^{2+} solution (Figure 6). The interaction of spermine and change in color of the solution of **O1**·Cu^{2+} can be explained on the basis that complexation of the copper ion with the of Schiff-base nitrogen atom[26] results in its characteristic peak at 397 nm, while its decomplexation on addition of spermine leads to disappearance of the peak, and complexation of **O1** with spermine leads to appearance of a new peak at 551 nm.

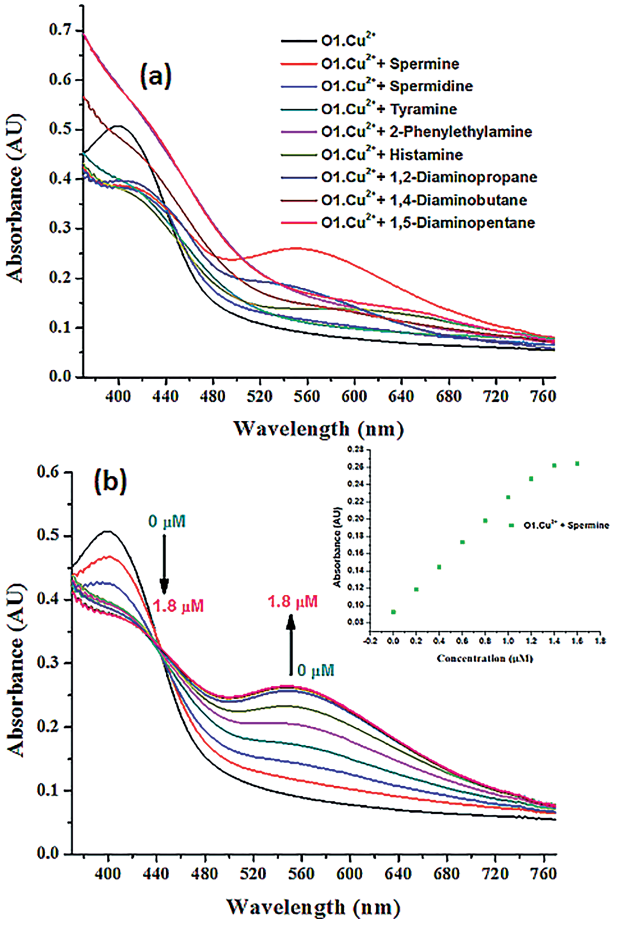

Figure 5. (a) Change in the UV/Vis absorption profile of **O1**·Cu^{2+} complex in the presence of different BAs (spermine, spermidine, tyramine, 2-phenylethylamine, histamine, 1,2-diaminopropane, 1,4-diaminobutane, and 1,5-diaminopentane; 100 µM each). (b) Change in the UV/Vis absorption profile of **O1**·Cu^{2+} complex with increasing concentration of spermine in the range 0–100 µM in aqueous medium. Inset: plot of absorbance as a function of the concentration of spermine in the range 0–1.6×10^{-6} M at λ_{max} = 551 nm.

Changes in the absorption intensity at 551 nm were linear with spermine concentration in the range of 0–1.6×10^{-6} M with a detection limit[25] for spermine of 7.62 nM. Additionally, **O1**·Cu^{2+} was found to be stable in aqueous environments in the pH range of 6–11. No substantial effect of ionic concentration on the profile of **O1**·Cu^{2+} was observed on successive addition of perchlorate salt (0–100 equiv.), which is proof of its potential under physiological conditions (Figures S8 and S9). To check its use as a real-time tool for determination of spermine, the time dependence of the interaction between **O1**·Cu^{2+} and

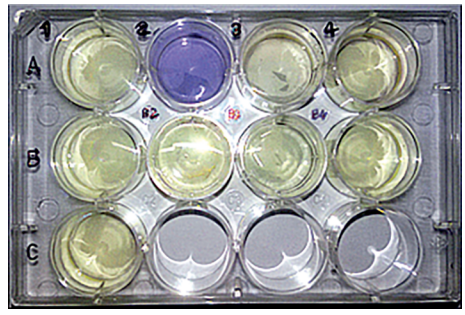

Figure 6. Change in the color of O1·Cu^{2+} solution on addition of 100 µM BA in aqueous medium. (A1) **O1**·Cu^{2+} only, (A2) **O1**·Cu^{2+} + spermine, (A3) **O1**·Cu^{2+} + spermidine, (A4) **O1**·Cu^{2+} + tyramine, (B1) **O1**·Cu^{2+} + 2-phenylethylamine, (B2) **O1**·Cu^{2+} + histamine, (B3) **O1**·Cu^{2+} + 1,2-diaminopropane, (B4) **O1**·Cu^{2+} + 1,4-diaminobutane, (C1) **O1**·Cu^{2+} + 1,5-diaminopentane.

spermine was recorded. Response-time studies were performed with additions of varying concentrations of spermine (0.2, 0.6, 1.0, and 1.4 mM) and the mixtures observed as a function of time. The interaction occurred within the first 3 min, and afterwards no change in absorption profile was observed up to 8 min (Figure 7).

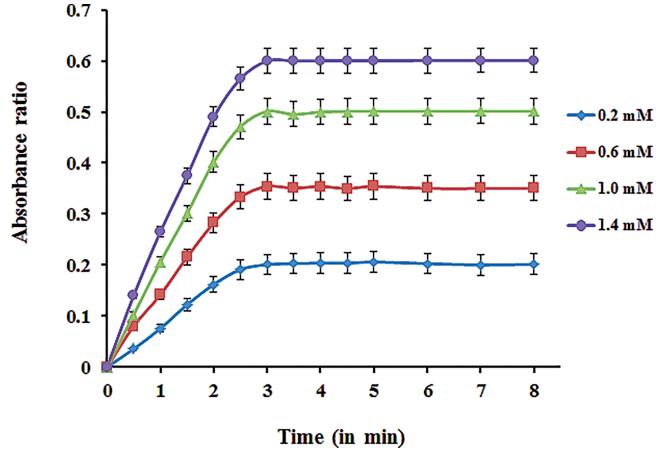

Figure 7. Response-time plot of **O1**·Cu^{2+} and spermine at varying concentrations of spermine (0.2, 0.6, 1.0, and 1.4 mM) in DMF/water (1/99, v/v) solvent system (λ_{max} = 551 nm).

Real-Sample Analysis

To test the applicability of the complex in real-time analysis, artificial samples with known concentrations of spermine were prepared. The prepared samples were screened with the proposed sensor (Table 1).

Table 1. Real-sample analysis of artificially prepared samples of spermine and percentage recoveries.

Sample	Concentration added [µM]	Concentration of spermine[a] [µM]	Recovery [%]
1	1	0.95 ± 0.02	95
2	1.5	1.47 ± 0.01	98
3	2	1.96 ± 0.05	98

[a] Mean of three determinations.

It is evident from Table 1 that the proposed sensor can determine spermine in solution with high accuracy and a percentage recovery of more than 95% in all samples.

Conclusions

Organic nanoaggregates were developed for selective chemosensing of spermine in aqueous medium. Contributing factors to the selective chemosensing of spermine are the weakly fluorescent complex of **O1**·Cu^{2+} with spermine, which induced changes in the color of the complex, and the UV/Vis spectral profile of **O1**·Cu^{2+}. Single-crystal XRD confirmed the interactions between binding sites of **1** and Cu^{2+}. Selective determination of spermine was achieved with a solution of **O1**·Cu^{2+}, which had a detection limit of 7.62 nM in the concentration range of 0–1.6×10^{-6} M.

Experimental Section

General Information: All chemicals used were of analytical grade and were purchased from Sigma-Aldrich Co. ^{1}H and ^{13}C NMR spectra were recorded with a JNM-ECS400 (JEOL) instrument operating at 400 MHz for ^{1}H and 100 MHz for ^{13}C. IR spectra were recorded with a Bruker Tensor 27 spectrometer on compounds in the solid state as KBr disks or as neat samples. CHN analysis was performed with a Flash EA 1112 elemental analyzer. UV/Vis spectral profiles were recorded with a Spectroscan 30. The particle size of nanoaggregates was determined by DLS with the external probe of a Metrohm Microtrac Ultra Nanotrac particle size analyzer. Fluorescence data were recorded with an RF-5301 PC spectrofluorometer, and mass spectra were recorded with a Waters Micromass Q-Tof mass spectrometer.

Synthesis of Receptor 1: Dipicolinic acid hydrazide (0.195 g, 1 mmol) and salicylaldehyde (0.244 g, 2.0 mmol) were heated to reflux in ethanol (50 mL). After 6 h, a yellow precipitate was obtained. The precipitate was collected by filtration and washed with ethanol, yield 72%. ^{1}H NMR (400 MHz, $CDCl_3$ + [D_6]DMSO): δ = 6.96–6.98 (m, 4 H, Ar), 7.34 (t, 2 H, Ar), 7.70 (d, 2 H, Ar), 8.29–8.33 (m, 1 H, Ar), 8.37–8.39 (d, 2 H, Ar), 8.94 (s, 2 H, N=CH),11.07 (s, 2 H, OH), 12.43 (s, 2 H, NH) ppm. ^{13}C NMR (100 MHz, $CDCl_3$ + [D_6]DMSO): δ = 116.5, 118.9, 119.6, 125.7, 129.0, 131.8, 140.0, 148.0, 149.2, 157.5, 159.4 ppm. IR (KBr): $\tilde{\nu}$ = 1682 (s), 2924 cm^{-1} (s). ESI-MS: *m/z* = 402.1 $[M - H]^+$. $C_{21}H_{17}N_5O_4$ (403.4): calcd. C 62.53, H 4.25, N 17.36; found C 62.48, H 4.31, N 17.41.

X-ray Crystallography: The diffraction data for single-crystal X-ray structure analysis of the copper complex were collected at 293 K with a Bruker X8 APEX II KAPPA CCD diffractometer by using graphite-monochromatized Mo-K_α radiation (λ = 0.71073 Å). The crystal was kept at 50 mm from the CCD, and measurements of diffraction spots were obtained with a counting time of 10 s. The APEX II program suite (Bruker, 2007) was employed for data reduction and multiscan absorption correction. The structure was solved by direct methods with the SIR97 program,[27] and full-matrix least-squares refinement was performed with SHELXL-97.[28]. Refinement of all non-H atoms was carried out anisotropically. The isotropic parameters of CH hydrogen atoms were 1.2 times those of the atoms to which they are attached. The remaining calculations were executed with the programs WinGX[29] and PARST,[30] and molecular diagrams were drawn with DIAMOND.[31] The crystallographic parameters, final *R* values, and refinement details are provided in Table S1. CCDC 1055494 contains the supplementary crystallographic data for this paper. These data can be obtained free of charge from The Cambridge Crystallographic Data Centre via www.ccdc.cam.ac.uk/data_request/cif.

Synthesis of Nanoaggregates: Organic nanoparticles were obtained by a single-step reprecipitation method. Working solutions of various concentrations were prepared by dissolving receptor **1** in DMF. The working solutions (0.5 mL) were used for formation of organic nanoparticles by slow injection into water (100 mL) with a microsyringe under sonication with continuous analysis of particle size by a DLS probe. Of the several concentrations used, the best-sized organic nanoparticles were formed at a concentration of 1 mM in DMF (1 mL). The thus-obtained organic nanoparticles (**O1**) were sonicated for a further 5 min while keeping the temperature of the solution at 25 ± 10 °C. Concentrations higher than the optimized concentration led to settling of the prepared organic nanoparticles due to agglomeration or large organic nanoparticles, even with continuous sonication. At concentrations lower than the optimum concentration, neither organic nanoparticles nor precipitates were formed.

Recognition Studies: UV/Vis absorption and fluorometric spectral profiles were recorded at 25 ± 1 °C. The solutions were shaken sufficiently and sonicated before recording the spectrum. The binding behavior of **O1** was first studied for various metal ions, and then the complex of **O2** with Cu^{2+} was used as a sensor by adding various BAs (100 μM) to solutions of **O1** (5 mL) in volumetric flasks. Before recording the spectra, the volumetric flasks were allowed to stand for 30 min. Titrations of **O1**·Cu^{2+} were performed by adding a solution of spermine to volumetric flasks containing a solution of **O1**·Cu^{2+} in aqueous medium. To determine the effect of ionic strength, the spectra were recorded at different concentrations of tetrabutylammonium perchlorate (0–100 equiv.). pH titrations were performed to explore the effect of pH on the recognition behavior by varying the acidity and basicity of the solution.

Real-Sample Analysis: Three different samples with known concentrations of spermine were prepared to test the real-time application of the proposed sensor.

Acknowledgments

This work was supported with research grant provided by Council of Scientific and Industrial Research (CSIR), New Delhi [project number 02(0216)/14/EMR-II] through project sanctioned to Dr. Navneet Kaur and Ms. Shweta Chopra is thankful to University Grants Commission (UGC), New Delhi for fellowships.

[1] A. Onal, *Food Chem.* **2007**, *103*, 1475–1486.
[2] N. Zhang, H. Wang, Z.-X. Zhang, Y.-H. Deng, H.-S. Zhang, *Talanta* **2008**, *76*, 791–797.
[3] T. L. Nelson, I. Tran, T. G. Ingallinera, M. S. Maynor, J. J. Lavigne, *Analyst* **2007**, *132*, 1024–1030.
[4] S. Shanmugan, K. Thandavan, S. Gandhi, S. Sethuraman, J. B. B. Rayappan, U. M. Krishnan, *Analyst* **2011**, *136*, 5234–5240.
[5] M. Venza, M. Visalli, D. Cicciu, D. Teti, *J. Chromatogr. B* **2001**, *757*, 111–117.
[6] M. J. Alkema, M. Hunter-Ensor, N. Ringstad, H. R. Horvitz, *Neuron* **2005**, *46*, 247–260.
[7] J. M. Landete, B. Rivas, A. Marcobal, R. Munoz, *Int. J. Food Microbiol.* **2007**, *117*, 258–269.
[8] S. Novella-Rodriguez, M. T. Veciana-Nogues, M. C. Vidal-Carou, *J. Agric. Food Chem.* **2000**, *48*, 5117–5123.

[9] A. Onal, S. E. K. Tekkeli, C. Onal, *Food Chem.* **2013**, *138*, 509–515.
[10] F. Kvasnicka, M. Voldrich, *J. Chromatogr. A* **2006**, *1103*, 145–149.
[11] C.-Y. Lu, H.-H. Su, Y.-L. Chen, W.-L. Tseng, *J. Chromatogr. A* **2014**, *1326*, 1–6.
[12] T. Li, H. Xie, Z. Fu, *Anal. Chim. Acta* **2012**, *719*, 82–86.
[13] G. Favaro, P. Pastore, G. V. Saccani, S. Cavalli, *Food Chem.* **2007**, *105*, 1652–1658.
[14] I. S. Park, E. Heo, Y.-S. Nam, C. W. Lee, J.-M. Kim, *J. Photochem. Photobiol. A: Chem.* **2012**, *238*, 1–6.
[15] J. Wang, Q. Zhang, Z. D. Liu, C. Z. Huang, *Analyst* **2012**, *137*, 5565.
[16] A. Singh, A. Singh, N. Singh, *Dalton Trans.* **2014**, *43*, 16283–16288.
[17] T. Pradhan, H. S. Jung, J. H. Jang, T. W. Kim, C. Kang, J. S. Kim, *Chem. Soc. Rev.* **2014**, *43*, 4684–4713.
[18] O. A. Ismail, M. A. Al-Omar, A. E.-G. E. Amr, *Curr. Org. Synth.* **2012**, *9*, 1–7.
[19] M. Liu, X. Zhang, B. Yang, Z. Li, F. Deng, Y. Yang, X. Zhang, Y. Wei, *Carbohydr. Polym.* **2015**, *121*, 49–55.
[20] X. Zhang, X. Zhang, B. Yang, Q. Chen, Y. Wei, *Colloids Surf. B* **2014**, *123*, 747–752.
[21] A. Kaur, T. Raaj, S. Kaur, N. Singh, N. Kaur, *Org. Biomol. Chem.* **2015**, *13*, 1204–1212.
[22] T. Asahi, T. Sugiyama, H. Masuhara, *Acc. Chem. Res.* **2008**, *41*, 1790–1798.
[23] Y. Hong, J. W. Y. Lam, B. Z. Tang, *Chem. Soc. Rev.* **2011**, *40*, 5361–5388.
[24] H. Lu, F. Su, Q. Mei, Y. Tian, W. Tian, R. H. Johnson, D. R. Meldrum, *J. Mater. Chem.* **2012**, *22*, 9890–9900.
[25] G. L. Long, J. D. Winefordner, *Anal. Chem.* **1980**, *52*, 2242–2249.
[26] A. Kuwar, R. Patil, A. Singh, S. K. Sahoo, J. Marek, N. Singh, *J. Mater. Chem. C* **2015**, *3*, 453.
[27] A. Altomare, M. C. Burla, M. Camalli, G. Cascarano, C. Giacovazzo, A. Guagliardi, A. G. G. Moliterni, G. Polidori, R. Spagna, *J. Appl. Crystallogr.* **1999**, *32*, 115–119.
[28] G. M. Sheldrick, *Acta Crystallogr., Sect. A* **2008**, *64*, 112–122.
[29] L. J. Farrugia, *J. Appl. Crystallogr.* **1999**, *32*, 837.
[30] M. Nardelli, *J. Appl. Crystallogr.* **1995**, *28*, 659.
[31] W. T. Pennington, *J. Appl. Crystallogr.* **1999**, *32*, 1028.

Received: May 6, 2015
Published Online: August 18, 2015

